Spontaneous emission of guided polaritons by quantum dot coupled to metallic nanowire: Beyond the dipole approximation

Ivan D. Rukhlenko,[1,*] **Dayan Handapangoda,**[1] **Malin Premaratne,**[1] **Anatoly V. Fedorov,**[2] **Alexander V. Baranov,**[2] **and Chennupati Jagadish**[3]

[1]*Department of Electrical and Computer Systems Engineering, Monash University, Clayton, Victoria 3800, Australia*
[2]*Center of Information Optical Technologies, State University of Information Technologies, Mechanics and Optics, St.-Petersburg 197101, Russia*
[1]*Department of Electronic Materials Engineering, Australian National University, Canberra, Australian Capital Territory 0200, Australia*
ivan.rukhlenko@eng.monash.edu.au

Abstract: In this paper, we theoretically analyze the emission of guided polaritons accompanying spontaneous recombination in a semiconductor quantum dot coupled to metallic nanowire. This study is aimed to shed light on the interaction between optically excited quantum emitters and metallic nanowaveguides beyond the validity of dipole approximation. To the best of our knowledge, this is the first time the geometry of quantum emitter and spatial inhomogeneity of the electric field constituting the fundamental polariton mode are fully taken into account. Even though we performed the analysis for disk-like quantum dot, all the conclusions are quite general and remain valid for any emitter with nanometer dimensions. Particularly, we found that the strong inhomogeneity of the electric field near the nanowire surface results in a variety of dipole-forbidden transitions in the quantum dot energy spectra. It was also unambiguously shown that there is a certain nanowire radius that gives maximum emission efficiency into the fundamental polariton mode. Since the dipole approximation breaks for nanowires with small radii and relatively big nanoemitters, the above features need to be considered in the engineering of plasmonic devices for nanophotonic networks.

OCIS codes: (240.5420) Polaritons; (230.5590) Quantum-well, -wire and -dot devices; (240.6680) Surface plasmons; (250.5403) Plasmonics; (230.7370) Waveguides; (350.4238) Nanophotonics and photonic crystals; (230.0250) Optoelectronics; (270.5585) Quantum information and processing; (040.6040) Silicon

References and links

1. H. Abdeldayem, D. O. Frazier, W. K. Witherow, C. E. Banks, B. G. Penn, and M. S. Paley, "Recent advances in photonic devices for optical super computing," in *Lecture Notes in Computer Science* **5172**, S. Dolev, T. Haist, and M. Oltean, eds. (Springer-Verlag, 2008), pp. 9-32.
2. H. A. Atwater, "The promise of plasmonics," Sci. Am. **296**, 56-63 (2007).

#114405 - $15.00 USD Received 17 Jul 2009; revised 9 Sep 2009; accepted 14 Sep 2009; published 16 Sep 2009

3. D. E. Chang, A. S. Sorensen, E. A. Demler, and M. D. Lukin, "A single-photon transistor using nanoscale surface plasmons," Nature Phys. **3**, 807-812 (2007).
4. S. A. Maier, "Plasmonics – towards subwavelength optical devices," Current Nanoscience **1**, 17-23 (2005).
5. W. L. Barnes, A. Dereux, and T. W. Ebbesen, "Surface plasmon subwavelength optics," Nature **424**, 824-829 (2003).
6. T. Thio, K. M. Pellerin and R. A. Linke, "Enhanced light transmission through a single subwavelength aperture," Opt. Lett. **26**, 1972-1974 (2001).
7. J. M. Raimond, M. Brune, and S. Haroche, "Manipulating quantum entanglement with atoms and photons in a cavity," Rev. Mod. Phys. **73**, 565-581 (2001).
8. T. W. Ebbesen, H. J. Lezec, H. F. Ghaemi, T. Thio, and P. A. Wolff, "Extraordinary optical transmission through sub-wavelength hole arrays," Nature **391**, 667-669 (1998).
9. H. Yokoyama, "Physics and device applications of optical microcavities," Science **256**, 66-70 (1992).
10. G. P. Agrawal, *Nonlinear Fiber Optics* (Academic, 2007).
11. E. Ozbay, "Plasmonics: Merging photonics and electronics at nanoscale dimensions," Science **311**, 189-193 (2006).
12. J. R. Krenn, B. Lamprecht, H. Ditlbacher, G. Schider, M. Salerno, A. Leitner, and F. R. Aussenegg, "Non-diffraction-limited light transport by gold nanowires," Europhys. Lett. **60**, 663-669 (2002).
13. K. Hennessy, A. Badolato, M. Winger, D. Gerace, M. Atature, S. Gulde, S. Falt, E. L. Hu, and A. Imamoglu, "Quantum nature of a strongly coupled single quantum dot-cavity system," Nature **445**, 896-899 (2007).
14. A. Wallraff, D. I. Schuster, A. Blais, L. Frunzio, R. S. Huang, J. Majer, S. Kumar, S. M. Girvin, and R. J. Schoelkopf, "Strong coupling of a single photon to a superconducting qubit using circuit quantum electrodynamics," Nature **431**, 162-167 (2004).
15. J. Takahara, S. Yamagishi, H. Taki, A. Morimoto, and T. Kobayashi, "Guiding of one-dimensional optical beam with nanometer diameter," Opt. Lett. **22**, 475-477 (1998).
16. S. A. Maier, "Plasmonics: The promise of highly integrated optical devices," IEEE J. Sel. Top. Quantum Electron. **12**, 1671-1677 (2006).
17. I. I. Smolyaninov, J. Elliott, A. Zayats, and C. C. Davis, "Far-field optical microscopy with a nanometer-scale resolution based on the in-plane magnification by surface plasmon polaritons," Phys. Rev. Lett. **94**, 057401 (2005).
18. A. V. Zayats and I. I. Smolyaninov, "Near-field photonics: Surface plasmon polaritons and localized surface plasmons," J. Opt. A: Pure Appl. Opt. **5**, S16-S50 (2003).
19. C. Untiedt, G. Rubio, S. Vieira, and N. Agraït, "Fabrication and characterization of metallic nanowires," Phys. Rev. B **56**, 2154-2160 (1997).
20. S. A. Maier and H. A. Atwater, "Plasmonics: Localization and guiding of electromagnetic energy in metal/dielectric structures," J. Appl. Phys. **98**, 011101 (2005).
21. S. A. Maier, "Plasmonics: Metal nanostructures for subwavelength photonic devices," IEEE J. Sel. Top. Quantum Electron. **12**, 1214-1220 (2006).
22. P. J. Pauzauskie and P. Yang, "Nanowire Photonics," Mater. Today **9**, 36-45 (2006).
23. M. Orrit, "Quantum light switch," Nature Phys. **3**, 755-756 (2007).
24. D. E. Chang, A. S. Sorensen, E. A. Demler, and M. D. Lukin, "Quantum optics with surface plasmons," Phys. Rev. Lett. **97**, 053002 (2006).
25. Y. N. Chen, G. Y. Chen, D. S. Chuu, and T. Brandes, "Quantum-dot exciton dynamics with a surface plasmon: Band-edge quantum optics," Phys. Rev. A **79**, 033815 (2009).
26. A. V. Akimov, A. Mukherjee, C. L. Yu, D. E. Chang, A. S. Zibrov, P. R. Hemmer, H. Park, and M. D. Lukin, "Generation of single optical plasmons in metallic nanowires coupled to quantum dots," Nature **450**, 402-406 (2007).
27. G. Y. Chen, Y. N. Chen, and D. S. Chuu, "Spontaneous emission of a quantum dot excitons into surface plasmons in a nanowire," Opt. Lett. **33**, 2212-2214 (2008).
28. D. E. Chang, A. S. Sorensen, P. R. Hemmer, and M. D. Lukin, "Strong coupling of single emitters to surface plasmons," Phys. Rev. B **76**, 035420 (2007).
29. E. M. Purcell, "Spontaneous emission probabilities at radio frequencies," Phys. Rev. **69**, 681-681 (1946).
30. D. Kleppner, "Inhibited spontaneous emission," Phys. Rev. Lett. **47**, 233-236 (1981).
31. Y. Yamamoto, S. Machida, and G. Björk, "Microcavity semiconductor laser with enhanced spontaneous emission," Phys. Rev. A **44**, 657-668 (1991).
32. M. Born and E. Wolf, *Principles of Optics* (Pergamon, 1986).
33. J. D. Jackson, *Classical Electrodynamics* (John Wiley & Sons, 1962).
34. J. A. Stratton, *Electromagnetic Theory* (McGraw-Hill, 1941).
35. A. V. Fedorov, A. V. Baranov, I. D. Rukhlenko, T. S. Perova, and K. Berwick, "Quantum dot energy relaxation mediated by plasmon emission in doped covalent semiconductor heterostructures," Phys. Rev. B **76**, 045332 (2007).
36. A. V. Baranov, A. V. Fedorov, I. D. Rukhlenko, and Y. Masumoto, "Intraband carrier relaxation in quantum dots embedded in doped heterostructures," Phys. Rev. B **68**, 205318 (2003).

#114405 - $15.00 USD Received 17 Jul 2009; revised 9 Sep 2009; accepted 14 Sep 2009; published 16 Sep 2009

37. L. D. Landau, E. M. Lifshitz, and L. P. Pitaevskii, *Course of Theoretical Physics, Vol. 8; Electrodynamics of Continuous Media* (Elsevier, 2004).
38. T. Laroche and C. Girard, "Near-field optical properties of single plasmonic nanowires," Appl. Phys. Lett. **89**, 233119 (2006).
39. T. Laroche, A. Vial, and M. Roussey, "Crystalline structure's influence on the near-field optical properties of single plasmonic nanowires," Appl. Phys. Lett. **91**, 123101 (2007).
40. N. Mori and T. Ando, "Electronoptical-phonon interaction in single and double heterostructures," Phys. Rev. B **40**, 6175-6188 (1989).
41. W. Murray and W. L. Barnes, "Plasmonic materials," Adv. Mater. **19**, 3771-3782 (2007).
42. M. Abramowitz and I. A. Stegun, *Handbook of Mathematical Functions* (Dover, 1964).
43. L. D. Landau and E. M. Lifshitz, *Course of Theoretical Physics, Vol. 3; Quantum Mechanics: Non-relativistic Theory* (Elsevier, 2003).
44. I. D. Rukhlenko, A. V. Fedorov, A. V. Baranov, T. S. Perova, and K. Berwick, "Tip-enhanced secondary emission of a semiconductor quantum dot," Phys. Rev. B **77**, 045331 (2008).
45. S. Scheel, L. Knöll, D.-G. Welsch, and S. M. Barnett, "Quantum local-field correlations and spontaneous decay," Phys. Rev. A **60**, 1590-1597 (1999).

1. Introduction

Subwavelength nanophotonics applications exceedingly demand the ability to operate with single light quanta and guide light far beyond the classical diffraction limit [1–9]. In order to gain full control over the light in nanoscales, engineers must devise efficient ways to extract optical energy from emitters, effectively guide it, and couple to the absorbers. In the standard fiber-optic communication systems, these problems are tackled by dielectric fibers or semiconductor waveguides [10]. However, natural limitation of the lateral dimensions of ordinary waveguides by the effective wavelength of light rule them out from applications in the subwavelength regime. Fortunately, an efficient transport of optical signals in nanoscale may be realized by metallic nanowires [11, 12]. Similar to fibers in macro-devices, metallic nanowires are able to provide strong coherent coupling with single-photon modes prevalent in nanophotonic networks [3, 13–15]. The essential properties of metallic nanowires stem from the interaction of electromagnetic field with electron density oscillations leading to the formation of quasiparticles, known as plasmon-polaritons. These quasiparticles propagate along the surface of nanowires and sometimes are referred to as surface plasmon-polaritons (SPP) in literature [16–18]. Given that the bulk plasmon-polaritons in nanowires does not exist, we use the term "polaritons" instead of SPP in this paper.

Regardless of the radius, metallic nanowire supports at least one polariton mode, which is spatially confined near its surface. Consequently, the energy of the optical field may be always transported along the metallic nanowire in the form of polaritons with prescribed localization determined by the nanowire radius. In combination with the possibility of precise metal fabrication on nanoscale [19], this feature makes nanowires especially attractive for quantum information technology [20, 21]. Particularly, the light channeled by nanowire polaritons may be employed to create two building blocks of nanophotonic circuits: subwavelength optical waveguides [15, 21, 22] and single-photon switches [2, 23]. For effective operation of these devices, a reliable conversion of light into guided polaritons and *vice versa* is needed as well as strong controllable coupling between nanowires and nanoemitters is required. The light-polaritons conversion may be realized, for example, by coupling of nanowire to dielectric waveguide [24], whereas the strong coupling of metallic nanowires to optical emitters is realizable owing to the ultra-small volumes of polariton modes [25].

Recently, it has been experimentally shown that the spontaneous emission of CdSe quantum dot may be almost entirely directed into the polaritons of silver nanowire with radius about 50 nm [26]. The high emission rate observed in this experiment has been theoretically investigated by two research groups [24, 25, 27, 28]. Analyzing the emission properties of a dipole emitter near a nanowire, they showed that the Purcell factor may exceed 500 upon the excita-

#114405 - $15.00 USD Received 17 Jul 2009; revised 9 Sep 2009; accepted 14 Sep 2009; published 16 Sep 2009

tion of the fundamental polariton mode [24] and is further enhanced for other modes because of their higher density of states [25]. In this paper, we abandon the dipole approximation used in these works to study in detail the polariton-mediated dynamics of the electronic subsystem of the emitter. We calculate analytically the generation rate of fundamental polaritons in metallic nanowire coupled to emitter of finite size. In the calculations, the emitter is modeled by a cylindrically-symmetric quantum dot in the strong confinement regime. The expression obtained is used to analyze the specific properties of polariton emission efficiency against dipole-allowed and dipole-forbidden transitions. We also consider the possibility to utilize the polariton emission for engineering of quantum dot electronic dynamics.

2. Fundamental polariton mode in a cylindrical metallic nanowire

The process of spontaneous recombination in a semiconductor quantum dot is caused by interaction of the quantum dot electronic subsystem with vacuum field fluctuations [29–31]. The intensity of these fluctuations is substantially enhanced in the vicinity of a conducting nanowire leading to the spontaneous recombination of electrons and holes (or excitons) with emission of guided polariton modes. To calculate the recombination rate associated with the spontaneous polariton emission, first we need to find the electromagnetic field generated by polaritons outside the nanowire. For this purpose, we consider nanowire as an infinitely long metallic cylinder with radius R and permittivity $\varepsilon_1(\omega)$ surrounded by a homogeneous dielectric with high-frequency permittivity ε_2 (see Fig. 1). The electromagnetic field and dispersion of polaritons propagating along the cylinder are determined by the solution of Maxwell's wave equation satisfying standard boundary conditions of classical electrodynamics [32–34]. The electric component of the field accompanying non-radiative polaritons with frequency ω and wave-vector k can be represented in the form

$$\mathbf{E}(\mathbf{r},t) = \sum_{m=-\infty}^{\infty} \mathbf{E}_m(\rho)\exp[i(kz-\omega t+m\varphi)] + \text{c.c.},$$

where $m \in \mathbb{Z}$, $\mathbf{E}_m(\rho)$ is the electric field vector of the mth polariton mode, and ρ, φ, and z are the cylindrical coordinates. We assume that the propagation is lossless and thus k values are real. In what follows, we only consider the cylinders whose radii satisfy the condition $R \ll |\kappa_j|^{-1}$, where $\kappa_j = \varepsilon_j^{1/2}\omega/c$, $j = 1,2$. We shall be referring to such cylinders as nanowires.

In the case of small nanowire radius, only a fundamental TE polariton mode with $m = 0$ is involved in the process of spontaneous emission. The other, "windy" modes are either not localized near the nanowire or experience a cutoff in the reciprocal space [28]. The amplitude of the fundamental polariton mode is given by [25]

$$\mathbf{E}_0(\rho) = E_0 \times \begin{cases} \eta\left[I_1(\alpha_1\rho)\mathbf{e}_\rho - i(\alpha_1/k)I_0(\alpha_1\rho)\mathbf{e}_z\right], & \rho \le R \\ K_1(\alpha_2\rho)\mathbf{e}_\rho - i(\alpha_2/k)K_0(\alpha_2\rho)\mathbf{e}_z, & \rho \ge R \end{cases} \tag{1}$$

where E_0 is the normalization constant, $\alpha_j = (k^2-\kappa_j^2)^{1/2}$ is the attenuation coefficient of the jth media, $I_n(x)$ and $K_n(x)$ are the modified Bessel functions of the first and second kinds, $\mathbf{e}_\rho$ and $\mathbf{e}_z$ are the unit vectors, and $\eta = -(\varepsilon_2/\varepsilon_1)K_1(\alpha_2 R)/I_1(\alpha_1 R)$. The constant E_0 can be found by applying the secondary quantization procedure [28, 35, 36]. In the case of dispersive media, this procedure leads to the equation [37]

$$\frac{1}{4\pi}\int \frac{\mathrm{d}(\omega\varepsilon)}{\mathrm{d}\omega}|\mathbf{E}_0(\rho)|^2 \mathrm{d}V = \hbar\omega, \tag{2}$$

where the integration is carried out over the whole space.

#114405 - $15.00 USD Received 17 Jul 2009; revised 9 Sep 2009; accepted 14 Sep 2009; published 16 Sep 2009

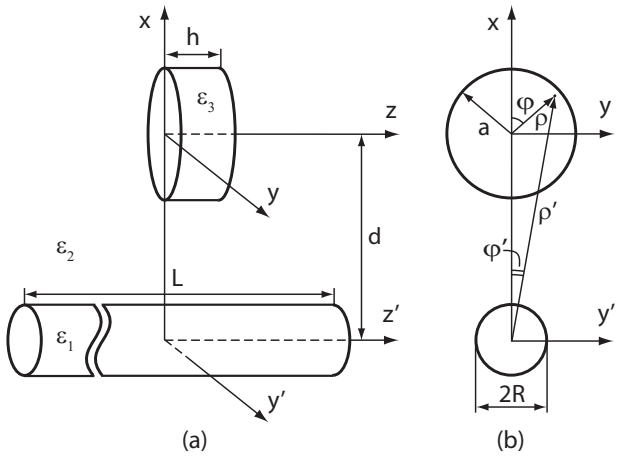

Fig. 1. The metallic nanowire and semiconductor quantum dot considered in the paper: (a) general view; (b) *xy*-plane projection. The permittivities of nanowire, surrounding media, and quantum dot are ε_1, ε_2, and ε_3, respectively; R and L are the radius and length of nanowire; a and h are the radius and height of quantum dot; d is the distance between the symmetry axes of quantum dot and nanowire.

To proceed further, we need to specify the frequency dependance of metal permittivity. According to the Drude dispersion model, the permittivity of metal at sufficiently high frequencies ($\omega < \omega_p$, ω_p is the plasma frequency) is predominantly real and can be written as

$$\varepsilon_1(\omega) \approx \varepsilon_\infty \left(1 - \frac{\omega_p^2}{\omega^2}\right).$$

For simplicity, we ignored the small imaginary part of ε_1 which is equivalent to the assumption of the infinite lifetime of polariton modes. This assumption is practically valid for real nanowires shorter than the polariton decay length, which is about tens of μm [28, 38, 39].

Using the above expression for $\varepsilon_1(\omega)$, we readily obtain from Eqs. (1) and (2)

$$E_0 = \left(\frac{2\hbar\omega}{\sigma L}\right)^{1/2}, \tag{3}$$

where L is the normalization length of nanowire and σ is the effective normalization area,

$$\sigma = \varepsilon_\infty \eta^2 \left(1 + \frac{\omega_p^2}{\omega^2}\right) \int_0^R \left[I_1^2(\alpha_1\rho) + (\alpha_1/k)^2 I_0^2(\alpha_1\rho)\right] \rho \, \mathrm{d}\rho + \varepsilon_2 \int_R^\infty \left[K_1^2(\alpha_2\rho) + (\alpha_2/k)^2 K_0^2(\alpha_2\rho)\right] \rho \, \mathrm{d}\rho.$$

The dispersion of fundamental polariton mode, $\omega(k)$, ensuring the continuity of z-component of the electric field (1), is implicitly given by the equation

$$\eta(\omega) = \frac{\alpha_2}{\alpha_1} \frac{K_0(\alpha_2 R)}{I_0(\alpha_1 R)}. \tag{4}$$

#114405 - $15.00 USD Received 17 Jul 2009; revised 9 Sep 2009; accepted 14 Sep 2009; published 16 Sep 2009

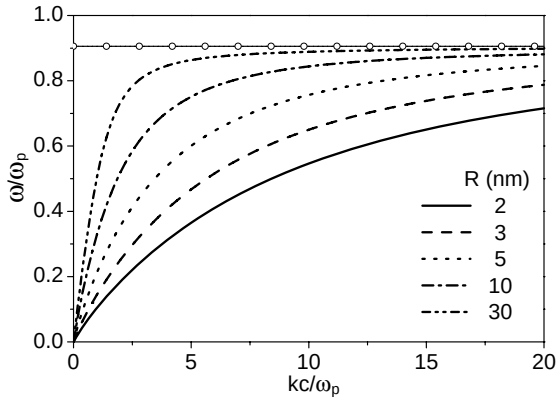

Fig. 2. The dispersion of fundamental polariton mode for different radii, R of silver nanowire embedded in SiO_2. The horizontal line with circle markers shows the saturation frequency $\omega(\infty) \approx 0.91\,\omega_p$. In the calculations, we used the following parameters: $\omega_p = 3.76$ eV, $\varepsilon_\infty = 9.6$, $\varepsilon_2 = 2.1$.

In this paper, we perform all the calculations for silver nanowire embedded in SiO_2. This system can be easily grown on silicon substrate with existing silicon technology. The typical dispersion curves corresponding to such nanowires with different radii are shown in Fig. 2. The saturation frequency of these curves can be found by noting that, in the limit $k \to \infty$, Eq. (4) reduces to the well-known dispersion relation of interface modes in single heterostructure, $\varepsilon_1 + \varepsilon_2 = 0$, which follows from dielectric consideration [40]. Assuming that ε_2 does not depend on frequency, we find the limiting frequency of fundamental polariton mode to be $\omega(\infty) = \omega_p(1 + \varepsilon_2/\varepsilon_\infty)^{-1/2}$. It is also readily seen that the full dispersion of surface polaritons in plane heterostructure, $(kc/\omega)^2 = \varepsilon_1\varepsilon_2/(\varepsilon_1 + \varepsilon_2)$ [5, 41], follows from Eq. (4) in the limit $R \to \infty$, since for big arguments $K_0(x) \sim K_1(x)$ and $I_0(x) \sim I_1(x)$ [42].

3. Spontaneous recombination in a semiconductor quantum dot mediated by polariton emission

If an excited quantum dot located near metallic nanowire, a spontaneous emission into nanowire polaritons may occur. This process is caused by interaction of quantum dot electrons with nanowire via electric field of polariton modes. In this section, we restrict our analysis to the emission process of fundamental polaritons, which are assumed to be only slightly perturbed by the quantum dot. The rate of spontaneous polariton emission due to the recombination of electrons in state i with holes in state f (or annihilation of exciton in the state i) is given by the Fermi's "golden rule" of quantum mechanics [43],

$$w_{if} = \frac{2\pi}{\hbar^2} \sum_f \sum_k |V_{if}(k)|^2 \delta[\Omega_{if} - \omega(k)], \tag{5}$$

where $V_{if}(k)$ is the matrix element of one-polariton interband transition with frequency Ω_{if}. The first summation in Eq. (5) is performed over the degenerate final states of the carriers. The second summation is carried over all possible values of plasmon wave-vectors and is replaced by integration as

$$\sum_k \to \frac{L}{2\pi} \int_0^{k_{\max}} \mathrm{d}k,$$

#114405 - $15.00 USD Received 17 Jul 2009; revised 9 Sep 2009; accepted 14 Sep 2009; published 16 Sep 2009

provided that we are only tracking polaritons propagating along the $+z$-direction. Without introducing substantial error, the maximum polariton wave-vector, $k_{\max}$, can be changed to ∞ because for high k, the electric field is low and the corresponding contribution of matrix element into the integral is negligible. Then, the integration over k can be evaluated using δ-function with the result

$$w_{if} = \frac{L}{\hbar^2} \sum_f |V_{if}(k_0)|^2 |\omega'(k_0)|^{-1}, \tag{6}$$

where k_0 is determined from the equation $\omega(k_0) = \Omega_{if}$ and the prime indicates differentiation with respect to k. Using Eq. (4) it is easy to show that

$$\omega'(k) = \frac{\varepsilon_1(\omega)(\alpha_1^2 \mathscr{K} - \alpha_2^2 \mathscr{I})\,\omega k}{2\varepsilon_\infty(\alpha_1\alpha_2)^2(\omega_p/\omega)^2 + \kappa_1^2(\omega)(\varepsilon_2\,\alpha_1^2 \mathscr{K} - \varepsilon_\infty \alpha_2^2 \mathscr{I})},$$

where

$$\mathscr{I} = 1 + \alpha_1 R\left[\frac{I_0'(\alpha_1 R)}{I_0(\alpha_1 R)} - \frac{I_1'(\alpha_1 R)}{I_1(\alpha_1 R)}\right], \quad \mathscr{K} = 1 + \alpha_2 R\left[\frac{K_0'(\alpha_2 R)}{K_0(\alpha_2 R)} - \frac{K_1'(\alpha_2 R)}{K_1(\alpha_2 R)}\right].$$

To relate the matrix element $V_{if}(k)$ to the electric field generated by polaritons, we consider the quantum dot made up from a semiconductor with either T_d or O_h symmetry. In this case, utilizing the effective mass approximation and a two-band model of semiconductors, one may show that [44]

$$|V_{if}(k)|^2 = 2\left(\frac{eP}{\varepsilon_3 \hbar \omega}\right)^2 \sum_{j=x,y,z} \left|\mathscr{E}_{if}^{(j)}(k)\right|^2. \tag{7}$$

Here e is the electron charge, P is the Kein's parameter, ε_3 is the high-frequency permittivity of quantum dot, x, y, and z are the principal crystallographic axes of quantum dot, and $\mathscr{E}_{if}^{(j)}(k)$ is the matrix element of the jth component of the electric field calculated on the envelope wave functions $\psi_\nu(\mathbf{r})$,

$$\mathscr{E}_{if}^{(j)}(k) = \int \psi_f^*(\mathbf{r}) E_j(\mathbf{r}) \psi_i(\mathbf{r})\, \mathrm{d}V. \tag{8}$$

In deriving Eq. (7), we also used the quasi-static approximation and neglected the magnetic field of polariton modes.

Without loss of generality, we may model the quantum dot by a disk-shaped potential well with infinite barriers. In the strong confinement regime, the state of electron (hole) in such a well is determined by a set of three quantum numbers, $n, m \in \mathbb{N}_1$ and $l \in \mathbb{Z}$. Let us denote by a and h, the radius and height of the quantum well, respectively. Then, in the coordinates associated with the center of the well's base, the normalized wave function corresponding to the state $\nu \equiv \{n, l, m\}$ has the form [44]

$$\psi_\nu(\mathbf{r}) = \left(\frac{2}{\pi a^2 h}\right)^{1/2} \frac{J_l(\gamma_{nl}\rho/a)}{J_{l+1}(\gamma_{nl})} \sin(\pi m z/h) \exp(il\varphi), \tag{9}$$

where $J_l(x)$ is the Bessel function of the first kind and γ_{nl} is its nth zero [i.e., $J_l(\gamma_{nl}) = 0$].

The energy of electron (hole) in a disk-shaped quantum dot depends on the value of γ_{nl}. Owing to the property $J_{-l}(x) = (-1)^l J_l(x)$, all the states (9) with $l \neq 0$ are doubly degenerate.

#114405 - $15.00 USD Received 17 Jul 2009; revised 9 Sep 2009; accepted 14 Sep 2009; published 16 Sep 2009

The frequency of polariton emitted by electron upon transition between states $i=\{n,l,m\}$ and $f=\{n',l',m'\}$ is determined by the energy conservation law,

$$\Omega_{if}=\frac{E_g}{\hbar}+\frac{\hbar}{2m_e^*}\left(\frac{\gamma_{nl}^2}{a^2}+\frac{\pi^2m^2}{h^2}\right)+\frac{\hbar}{2m_h^*}\left(\frac{\gamma_{n'l'}^2}{a^2}+\frac{\pi^2m'^2}{h^2}\right),$$

where E_g is the bandgap and $m_{e(h)}^*$ is the effective mass of electron (hole). One important point to remember is that the above description of the quantum dot electronic subsystem in terms of noninteracting electrons and holes is valid until the dot size is much smaller than the exciton Bohr radius, i.e., when $\max\{a,h\}\ll R_{\rm ex}=\varepsilon_0\hbar^2/(\mu e^2)$, where ε_0 is the static permittivity of the quantum dot and $\mu=m_e^*m_h^*/(m_e^*+m_h^*)$.

For the sake of simplicity, we assume that the symmetry axes of quantum dot and nanowire are parallel to each other and separated by a distance d (see Fig. 1b). Using Eqs. (1), (8), and (9), it is easy to show that

$$\left|\mathscr{E}_{if}^{(j)}(k)\right|^2=E_0^2\Delta_{mm'}(kh)\sum_{j=x,y,z}\left|G_{nln'l'}^{(j)}(k)\right|^2,$$

where

$$\Delta_{mn}(x)=2F_{mn}^2(x)[1-(-1)^{m+n}\cos x],\quad F_{mn}(x)=\frac{4\pi^2mnx}{(2\pi^2mn)^2-[\pi^2(m^2+n^2)-x^2]^2},$$

$$G_{nln'l'}^{(x)}(k)=\frac{1}{\pi a^2}\int_0^a\rho\,\mathrm{d}\rho\int_0^{2\pi}\mathrm{d}\varphi\,K_1[\alpha_2\rho'(\rho,\varphi)]C(\rho,\varphi)\Phi_{nln'l'}(\rho)\exp[i(l-l')\varphi],$$

$$G_{nln'l'}^{(y)}(k)=\frac{1}{\pi a^2}\int_0^a\rho\,\mathrm{d}\rho\int_0^{2\pi}\mathrm{d}\varphi\,K_1[\alpha_2\rho'(\rho,\varphi)]S(\rho,\varphi)\Phi_{nln'l'}(\rho)\exp[i(l-l')\varphi],$$

$$G_{nln'l'}^{(z)}(k)=\frac{1}{\pi a^2}\int_0^a\rho\,\mathrm{d}\rho\int_0^{2\pi}\mathrm{d}\varphi\,K_0[\alpha_2\rho'(\rho,\varphi)](\alpha_2/k)\Phi_{nln'l'}(\rho)\exp[i(l-l')\varphi],$$

$$\rho'(\rho,\varphi)=\sqrt{(d+\rho\cos\varphi)^2+(\rho\sin\varphi)^2},\quad \Phi_{nln'l'}(\rho)=\frac{J_l(\gamma_{nl}\rho/a)J_{l'}(\gamma_{n'l'}\rho/a)}{J_{l+1}(\gamma_{nl})J_{l'+1}(\gamma_{n'l'})},$$

$$C(\rho,\varphi)=\frac{d+\rho\cos\varphi}{\rho'(\rho,\varphi)},\quad S(\rho,\varphi)=\frac{\rho\sin\varphi}{\rho'(\rho,\varphi)}.$$

Substituting this result in Eq. (7), we obtain from Eq. (6) the rate of spontaneous polariton emission in a fixed direction of nanowire,

$$w_{if}=w_{\rm rad}\frac{3\chi(l')c^3}{2\sigma\Omega_{if}^2\varepsilon_3^{5/2}}\frac{\Delta_{mm'}(k_0h)}{\omega'(k_0)}\sum_{j=x,y,z}\left|G_{nln'l'}^{(j)}(k_0)\right|^2,\tag{10}$$

where $w_{\rm rad}=8e^2P^2\Omega_{if}\varepsilon_3^{1/2}/(3\hbar^3c^3)$ is the radiative recombination rate [45], $\chi(l')=2-\delta_{l'0}$ takes into account double degeneracy of the final states with $l'\neq0$, and the values of all k-dependant quantities must be taken at $k=k_0$. We suppose in Eq. (10) that nanowire just slightly modifies the efficiency of radiative recombination and therefore $w_{\rm rad}$ does not depend on d. It is also worth noting that the electron-hole recombination rate with emission of polaritons propagating towards either of the nanowire ends is equal to $2w_{if}$.

Equation (10) constitutes the main result of our paper. According to Eq. (10), the polariton emission is possible upon transitions between any states with $\Omega_{if}<\omega(\infty)$. As can readily be

#114405 - $15.00 USD Received 17 Jul 2009; revised 9 Sep 2009; accepted 14 Sep 2009; published 16 Sep 2009

observed, this is a consequence of spatial inhomogeneity of electric field accompanying the fundamental polariton mode.

The emission rate of point dipole can be obtained from Eq. (10) as a passage to the limit when the quantum dot dimensions tend to zero ($a, h \to 0$), while the frequency Ω_{if} is fixed. In this case, it is easy to verify that $\Delta_{mm'}(0) = \delta_{mm'}$ and the sum in Eq. (10) reduces to $[K_1^2(\alpha_2 d) + (\alpha_2/k)^2 K_0^2(\alpha_2 d)]\delta_{nn'}\delta_{ll'}$. Thus, we come to the selection rule which is general for dipole approximation: only the transitions between states with the same quantum numbers are possible. The other well-known feature of polariton emission by point dipole located in the proximity of metallic nanowire is the $1/R^3$-divergency of the emission rate as the nanowire radius tends to zero [28]. To examine the scenario of small R in Eq. (10), we notice that for $R \to 0$, $\alpha_1 \approx \alpha_2 \approx k$. Further, the dispersion law (4) requires $kR = \vartheta_{if}$, where ϑ_{if} is a constant which depends only on polariton frequency. With this result, one may check that $\omega'(k_0) \propto R$ and $\sigma \propto R^2$. Finally, for $d \sim R$ from Eq. (10) we obtain

$$\lim_{R\to 0}\left(\lim_{\substack{a\to 0\\ h\to 0}} w_{if}\right) \propto \frac{\delta_{nn'}\delta_{ll'}\delta_{mm'}}{R^3}.$$

Physically, the divergency of the polariton emission rate as $R \to 0$ originates from neglecting the ohmic losses described by the imaginary part of ε_1. As we shall see in the next section, for emitters with finite dimensions, this divergency is absent even in nondissipative case.

It is worth noting that the above analysis may be easily extended to account for losses in the metal. These losses are characterized by an imaginary part of metal permittivity and result in complex-valued polariton dispersion, $\omega(k) = \omega'(k) + i\omega''(k)$ ($\omega'' > 0$), which implies the finite lifetime of polariton modes $\tau = 1/\omega''$. In the case of ultrathin nanowires, the imaginary part of the fundamental polariton frequency is known to be much smaller than the real part [27]. Therefore, one may introduce the effect of finite polariton lifetime into the equation for spontaneous emission rate by replacing Dirac's δ-function in Eq. (5) with the standard Lorenzian [35],

$$\delta[\Omega_{if} - \omega(k)] \to \frac{1}{\pi}\frac{\omega''}{(\Omega_{if} - \omega')^2 + \omega''^2},$$

and using only the real part of the polariton dispersion in the subsequent calculations. However, it is to be emphasized that such a formulation will not change the qualitative behavior of the spontaneous emission process described in Eq. (10).

4. Numerical examples and discussion

In this section, we illustrate the peculiarities of polariton emission by considering an InAs-quantum dot with the following parameters: $E_g = 414$ meV, $\varepsilon_3 = 12.25$, $m_e = 0.024\,m_0$, $m_h = 0.33\,m_0$, where m_0 is the free electron mass. The efficiency of recombination channel due to excitation of the fundamental polaritons propagating in $+z$ direction is characterized by the ratio of w_{if} to the sum of radiative and nonradiative recombination rates. Supposing that the quantum yield of the quantum dot in the absence of nanowire is close to 100%, we may define the efficiency of emission into the fundamental polariton mode with fixed propagation direction as

$$\beta_0 = \frac{1}{1 + w_{\mathrm{rad}}/w_{if}}.$$

Figure 3 shows the efficiency of spontaneous polariton emission upon the transitions allowed in the dipole approximation. The upper panel shows the variation of emission efficiency

#114405 - $15.00 USD Received 17 Jul 2009; revised 9 Sep 2009; accepted 14 Sep 2009; published 16 Sep 2009

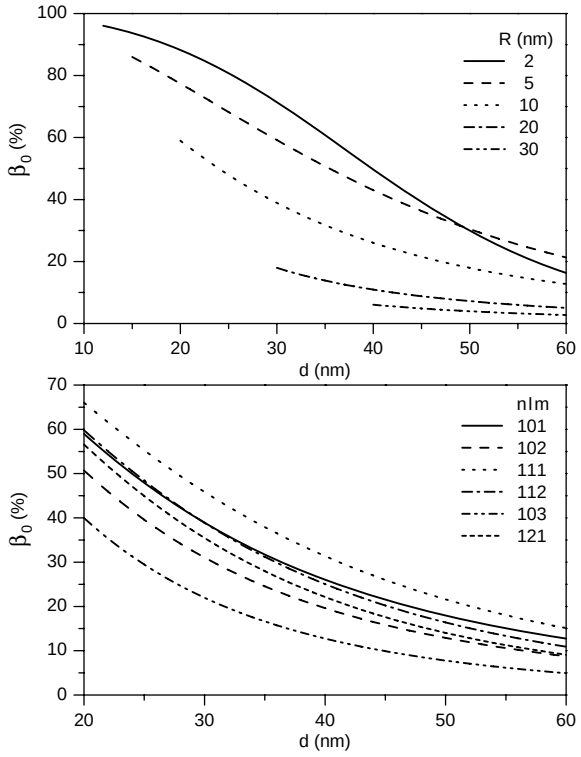

Fig. 3. The efficiency of guided polariton emission as a function of distance, d between the quantum dot and nanowire for dipole-allowed transitions with quantum numbers $\{n,l,m\} = \{n',l',m'\}$. In the upper panel, $n = 1$, $l = 0$, $m = 1$; in the lower panel, $R = 10$ nm; in both panels, $h = 2a = 20$ nm. For other parameters see the text.

with distance between the quantum dot and nanowire for different nanowire radii. It corresponds to the transition between ground states of electrons and holes in the quantum dot with $h = 2a = 20$ nm. One can see that for small nanowires, the emission efficiency may exceed 90%. This fact suggests ultrathin nanowires as a promising candidates for coupling of quantum emitters separated by distances of order of several μm. Both the quantum dot-nanowire interaction strength and its decay with distance decrease with increasing nanowire radius. Owing to the broad dispersion of the fundamental polariton mode, the emission upon the higher-energy transitions may also be very efficient. This is illustrated by the lower panel of Fig. 3.

The dependance of emission efficiency on nanowire radius for quantum dot touching the nanowire is presented in Fig. 4. The upper and lower panels correspond to the dipole-allowed and dipole-forbidden transitions, respectively. From these panels, we notice that metallic nanowire with $R \sim 2-3$ nm is capable of realizing more than 80%-coupling between single emitters attached to its surface. It is also seen that the emission efficiency initially grows with reducing of R, peaks for nanowires with radii below 2 nm, and then starts decaying to zero as $R \to 0$. This behavior is in striking distinction from the monotonous bent of β_0 to unity, which follows from the divergency of spontaneous emission rate deduced in the dipole approximation. The reason behind this difference is clear: even though the electric field of nanowire tends to infinity as R approaches zero, its strong localization results in negligible polariton emission by any emitter with finite dimensions.

Several qualitative conclusions can be made by comparing the panels of Fig. 4. First, the

#114405 - $15.00 USD Received 17 Jul 2009; revised 9 Sep 2009; accepted 14 Sep 2009; published 16 Sep 2009

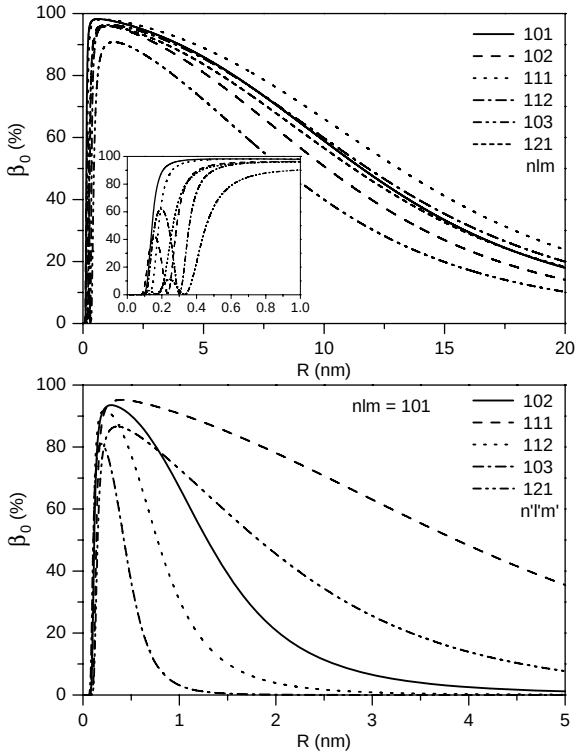

Fig. 4. The efficiency of guided polariton emission as a function of nanowire radius, R for dipole-allowed (upper panel) and dipole-forbidden (lower panel) transitions. The inset shows small-scale variation of the emission efficiency. In the calculations, it was assumed that the quantum dot with $h = 2a = 20$ nm touches the nanowire such that $d(R) = R + a$. The other parameters are the same as in Fig. 3.

polariton emission efficiency upon the dipole-allowed transitions decays much slower than that of the dipole-forbidden transitions. Particularly, for nanowire with $R = 10$ nm, the former is within the range $50-80\%$, whereas the latter is almost negligible. This is just a reflection of the fact that the electric field inhomogeneity grows with the increasing curvature of nanowire surface. Second, as $R \to 0$, the emission efficiency approaches zero exhibiting an infinite number of oscillations with a rapidly damped amplitude. In the inset of Fig. 4, several first peaks of these oscillations can be seen. The oscillations are governed by the function $\Delta_{mm'}(k_0 h)$ and result in zero emission efficiency for $R_q \approx \vartheta_{if} h/|x_q|$, where $x_q = (2q - m - m')\pi$ is the root of equation $\Delta_{mm'}(x) = 0$, $q \in \mathbb{N}$, and $q \neq \{0, m, m', m + m'\}$. Finally, the decay rate of emission efficiency is nearly the same in the upper panel for dipole-allowed transitions but substantially differs for dipole-forbidden transitions in the lower panel. In the latter case, the decay rate is determined by the quantum numbers m and m' of the states involved in the transition.

Figure 5 illustrates the variation of emission efficiency upon changes in the dimensions of the quantum dot with fixed volume. One can see that alteration of the quantum dot shape can be used to increase the polariton emission for some interband transitions and decrease it for the other. For example, only transitions between states with quantum numbers $\{1,0,1\}$, $\{1,1,1\}$, and $\{1,2,1\}$ are allowed if $h = 5$ nm. However, if the quantum dot height is increased up to 16 nm, three new transitions with quantum numbers $\{1,0,2\}$, $\{1,1,2\}$, and $\{1,0,3\}$ arise, whereas the transitions between states $\{1,2,1\}$ becomes nearly prohibited. At the same time,

#114405 - $15.00 USD Received 17 Jul 2009; revised 9 Sep 2009; accepted 14 Sep 2009; published 16 Sep 2009

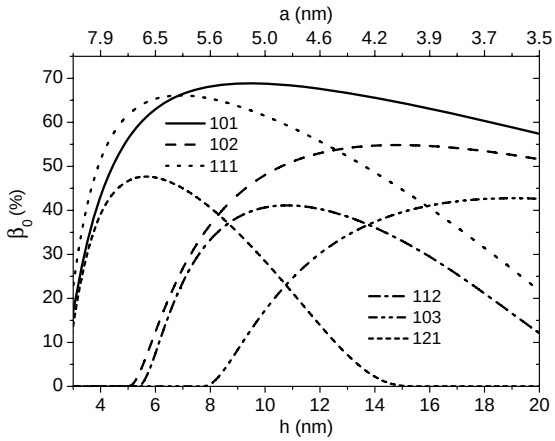

Fig. 5. The dependance of polariton emission efficiency on the quantum dot height, h (radius, a) for dipole-allowed transitions. The quantum dot volume was fixed with $a^2h = 250$ nm^3; $d = 15$ nm, $R = 5$ nm. The other parameters are the same as in Fig. 4.

the efficiency of the fundamental transition (solid curve) remains almost unchanged. Thus, the distinct dependencies of the polariton emission efficiency upon different interband transitions on nanowire radius and quantum dot dimensions offer wide opportunities to control the dynamics of optically excited quantum dots by suppressing or enhancing the specific transitions.

As a closing note, we would like to emphasize that the above analysis can be readily performed for either emitters of more complicated shapes or other nanowire geometries. The resulting information is necessary for better understanding of quantum dynamics of optoelectronic devices with subwavelength dimensions.

5. Conclusion

In conclusion, we have analytically investigated the process of energy relaxation in a semiconductor quantum dot accompanied by spontaneous emission of fundamental polariton modes of a metallic nanowire. We have found that the emission efficiency in quantum dots contacting ultrathin nanowires may exceed 90% for both dipole-allowed and dipole-forbidden transitions. Together with the weak out-coupling into free-space modes, which is inherent to ultrathin nanowires, this feature can be used to achieve the long-range coupling between distant quantum emitters. The distinct dependencies of emission efficiencies upon different interband transitions on nanowire radius and quantum dot dimensions have been suggested for the engineering of quantum dot electronic dynamics. We have also shown that the polariton generation rate is not only limited by the ohmic losses of metal but also by the finite size of the emitter.

Acknowledgment

This work was funded by the Australian Research Council through its Discovery Grant scheme under grant DP0877232. The work of A. V. Fedorov and A. V. Baranov was partially supported by the Federal Agency for Education of the Russian Federation (Grants Nos 2.1.1/1933 and 2.1.1/1880). C. Jagadish gratefully acknowledges Australian Research Council for financial support.

#114405 - $15.00 USD Received 17 Jul 2009; revised 9 Sep 2009; accepted 14 Sep 2009; published 16 Sep 2009